Available online at www.sciencedirect.com
SCIENCE DIRECT
Polymer 47 (2006) 5566–5573
polymer
www.elsevier.com/locate/polymer

In situ atomic force microscopy of the melting of melt-crystallized polyethylene

J.K. Hobbs [1]

Department of Chemistry, University of Sheffield, Brook Hill, Sheffield S3 7HF, UK

Received 28 January 2005; accepted 18 February 2005
Available online 11 May 2006

Abstract

High temperature AFM is used to observe the melting of polyethylene lamellae crystallized from the melt in situ in real-time. Both oriented and un-oriented samples are observed. The melting of shish–kebab structures, including revealing the bare oriented shish, is achieved. Lamellae are observed to melt from their edges, and this is proposed to be due to the inherent higher mobility at the crystal edges rather than differences in stability within the crystal due to different levels of post crystallization perfecting. Observation of the melting of structures that have been observed during growth confirms that material crystallized at lower temperatures melts first, followed by material crystallized in confined geometries, and finally the rest of the isothermally crystallized lamellae that melt back from the edges with an apparently random morphology that is not the reverse of the growth process. In situ observation during melting is confirmed as an alternative and complementary technique to etching to reveal behaviour during crystallization when crystallization is too rapid for in situ observation.

Keywords: Atomic force microscopy; Polyethylene; Melting

1. Introduction

Melt crystallized polymers have a highly complex morphology with a hierarchy of structures at different length scales controlled largely by the kinetics of the crystallization process [1]. Over the last 25 years the lamellar scale morphology of many polymers has been elucidated by electron microscopy, primarily through the use of the etching and replication techniques pioneered by Bassett et al. [2–4]. More recently, the same approach has been used to investigate how these structures are formed through careful use of quenching and extracting techniques [5,6]. The structure of melt crystallized polymers is now well understood, and although key questions remain to be answered in the crystallization process itself, this is arguably now the domain of theoreticians considering the wealth of experimental information available.

There are two areas where ex situ study is unable to provide unambiguous information. The nature of the growth front itself is hard to ascertain, as the quenching process will lead to decoration by material crystallized at lower temperatures, and it is probably not possible to discern between this and the initially crystallized (and probably less stable) material that is formed directly at the growing crystal front. Secondly, the melting of polymers is particularly difficult to study by ex situ methods for similar reasons—unambiguous identification of the material present at high temperature is at best problematic.

Over the last 10 years the development of scanning probe techniques such as atomic force microscopy (AFM) capable of in situ observation of polymer crystallization and melting, has led to several new insights into these processes, e.g. [7–12]. Although limited to the examination of the surface and near surface regions, the advantages afforded by in situ observation are considerable and are only just beginning to be explored. The melting and high temperature annealing of several polymers has been previously studied by AFM, e.g. [13–17]. In most cases isothermal melting or annealing has been carried out, due to the relatively slow rate at which AFM images are obtained, making direct comparison with the body of available thermal information on melting problematic. Polyethylene has primarily been investigated through the study of single crystals grown from dilute solution and deposited onto surfaces. These form ideal samples for AFM study, as the sample is well defined and the crystallography can be ascertained from the shape of the initially deposited crystal (one of the main disadvantages of AFM is the lack of crystallographic

E-mail address: Jamie.hobbs@sheffield.ac.uk.
[1] Much of this work was carried out at H.H. Wills Physics Department, University of Bristol, Tyndall Avenue, Bristol BS8 1TL, UK.

0032-3861/$ - see front matter © 2006 Elsevier Ltd. All rights reserved.
doi:10.1016/j.polymer.2005.02.133

information, available to TEM through diffraction). Some initial work on the melting of melt-crystallized polyethylene has been published [18], but here a broader overview will be presented, including the melting of both quiescent and oriented structures.

2. Experimental details

A sharp fraction of polyethylene obtained from the National Bureau of Standards, M_w 119600, M_w/M_n 1.1, was used throughout this study. Samples were initially cast from dilute solution in xylene onto hot glass slides to obtain thin films. To obtain oriented structures, a razor blade was dragged across the sample surface at a temperature of 140 °C, prior to cooling to the crystallization temperature, the same technique as used in [12]. To compare the effect of crystallization temperature on melting behaviour, the thin films were first melted at a temperature of 160 °C before transferring to a Linkam optical microscope hotstage pre-heated to the required crystallization temperature, where the sample was left until there were no further signs of crystallization in the optical microscope, and then quenched to room temperature. Subsequent melting experiments were carried out in situ in the AFM.

A Digital Instruments—Veeco Dimension 3100 AFM was used. This is a tip-scanned device that provides sufficiently large sample space to allow the use of a conventional Linkam hot-stage. The same AFM set-up was used as described previously [19], and the same problems relating to the exact calibration of the sample temperature apply. The temperature can be approximately calibrated from the observed melting temperature, although as melting occurs over a range of temperature, and the measured properties are different with different techniques (even when comparing optical microscopy to AFM), this is not entirely accurate. Also, as the temperature gradient doubtless changes with temperature (most probably becoming steeper as the nominal surface temperature is increased), this one point calibration cannot be relied on. However, considering the necessary variations in experimental set-up between experiments, a more exact technique could not be found. So, the temperatures quoted are indicative rather than absolute values. Imaging conditions were maintained so as to just enable the sample to be imaged, without damaging or interfering with the surface in any discernable way. Where mentioned below, an Infinitesima ActivResonance Controller was used to reduce the effective quality factor of the cantilever so as to allow faster image speeds to be obtained. This approach when applied to polymer crystallization and melting studies is discussed in detail in [20].

For melting studies samples were heated at a maximum rate of 1 °C/min. This is sufficiently slow that it was possible to obtain consecutive images of the same area during melting, and hence to offset subsequent images so as to maintain imaging over the same features on the sample, correcting for sample drift. Wherever possible scans are displayed with the same slow scan direction (i.e. up or down) as this maintains the same form to any distortion in the image due to drift on heating. In all cases topography, phase and amplitude images were obtained simultaneously. Where topographic images have been used, they are displayed with a slight tilt so as to facilitate the easy interpretation of the images. It was found that the topography images were less affected by the variations in the imaging cantilever's resonant frequency that occurs during heating than phase images. Although the cantilever was tuned close to the surface at the starting temperature of a heating run, slight

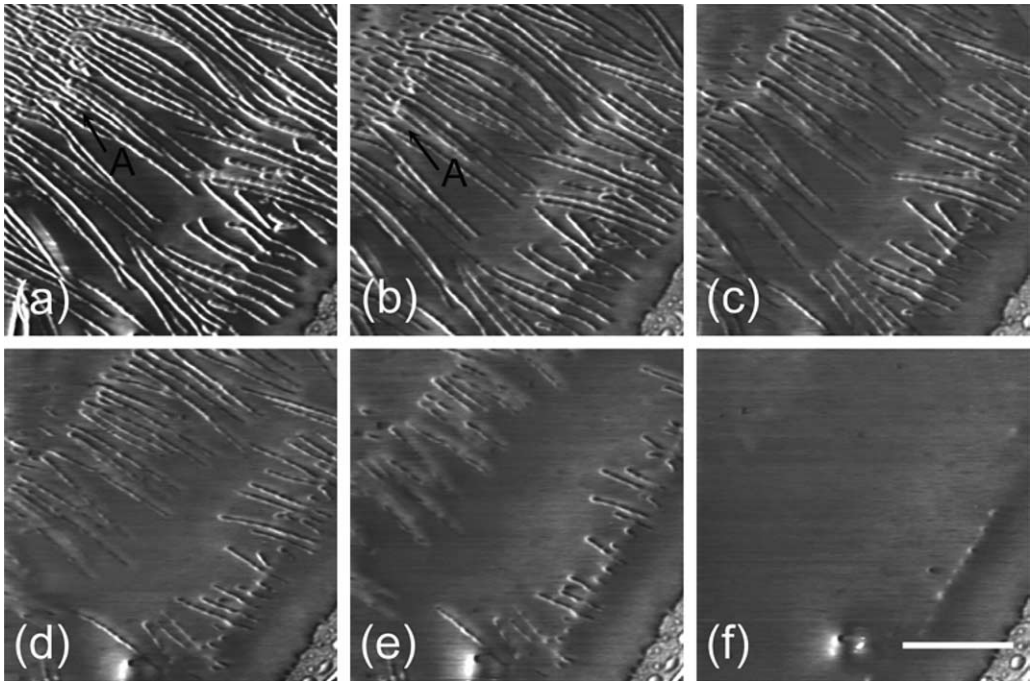

Fig. 1. A series of AFM phase images showing the gradual melting of an interlocking pair of shish–kebab structures at a heating rate of 1°C/min. (a) 129 °C, (b) 133.7 °C, (c) 134.7 °C, (d) 135.2 °C, (e) 135.6 °C, (f) 136.5 °C. Black to white represents a change of phase of 50°. The scale bar represents 1 μm.

variations in resonant frequency cause a change in the position of the cantilever's phase response, which can cause degradation in the phase image when collected over the wide range of temperatures necessary for some of the studies detailed here.

3. Results

Fig. 1 shows a series of images taken during the gradual heating of an oriented structure. This is the same sample that is shown crystallizing in the supplementary information provided in [21]. Initial crystallization occurred at a ~129 °C, and the sample was then heated without cooling further so as to follow the melting of this material. The oriented shish are not visible in these images, but the growth of lamellae that are strictly aligned perpendicular to the sample surface is apparent. The sample was heated at a constant rate of 1 °C/min. The effective quality factor (Q) of the cantilever was reduced from its natural value of ~300 to ~80 for these images. This reduction in the effective Q causes a reduction in the contrast obtained in the phase image, and here, due to the very fast scan rates used (line rate 10 Hz) the data cannot be interpreted in terms of the material properties of the sample as it is heavily convoluted with topographic information. However, the distinction between crystalline and amorphous material is clear. The lamella labelled A that crystallized under the constraint of neighbouring lamellae, can be seen to melt out during the early stages of heating. Topographically, the area shown in these images lies on ridge of molten polymer approximately 100 nm thick that was formed by the motion of the orienting razor blade, and the height rapidly decreases to the substrate on the top left and bottom right of the image. The morphology is clearly constrained by this limited film thickness.

Fig. 2 shows the final stages of melting of a bundle of shish–kebab structures. Here, the film thickness was approximately 300 nm. The sample was heated at 0.5 °C/min. The stability of the set-up was not optimised, and sample drift within images can be seen as slight kinks in the shish structures (example arrowed in Fig. 2(d))—these are artefacts of the imaging. The shish backbones can be clearly seen with incipient lamellar overgrowths that appear as oval regions fairly regularly spaced along the backbones. These lamellae gradually melt back during the slow heating process to leave the bare backbones, which then melt on further heating. The time resolution is insufficient to obtain images of the shish melting—they disappear between scans.

Fig. 3 shows a topographic image of a crystal aggregate grown at ~127 °C, imaged at the crystallization temperature prior to cooling. The crystal has grown from an un-oriented melt. The featureless areas around the periphery of the image are molten polymer. After crystallizing to the extent shown, the sample was then cooled (while still imaging) to 112 °C before

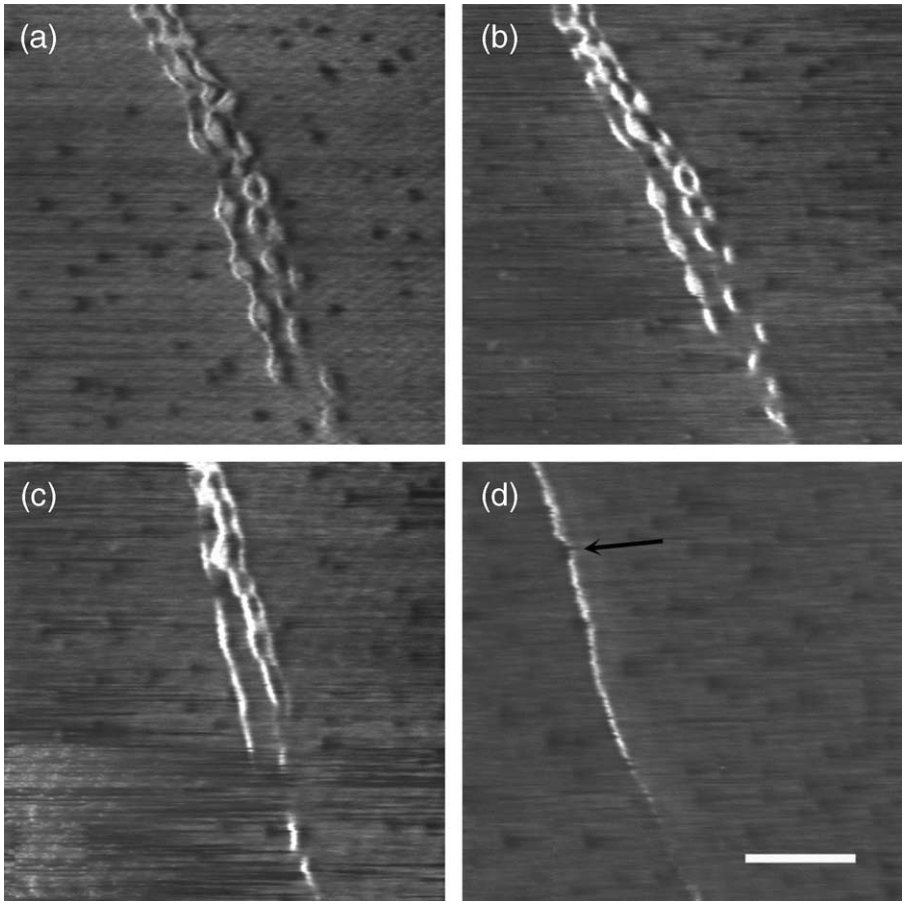

Fig. 2. A series of AFM phase images showing the gradual melting during heating at 0.5 °C/min of the extended chain shish structures. (a) 136.8 °C, (b) 139.1 °C, (c) 141.4 °C, (d) 143.7 °C. Black to white represents a change in phase of 70°. The scale bar represents 250 nm.

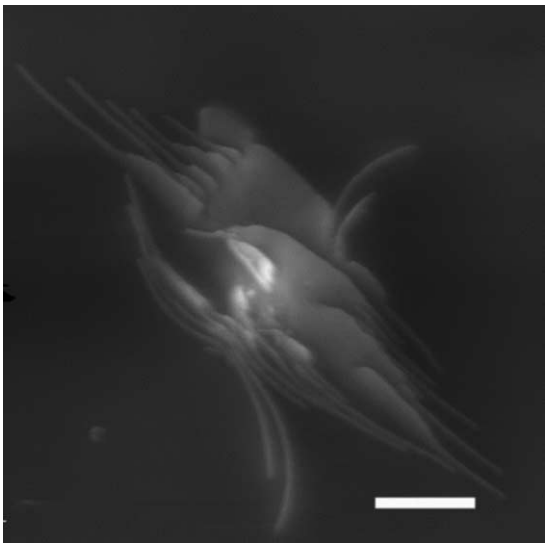

Fig. 3. A topographic AFM image showing a crystal aggregate at 127 °C following crystallization at that temperature. The image has been tilted slightly to enhance contrast. Black to white represents a variation in height of 200 nm. The scale bar represents 1 μm.

re-heating to 126 °C and then heating at 1 °C/min to the melting temperature. The gradual melting of the aggregate is shown in Fig. 4. Fig. 4(a) shows the sample prior to the onset of melting, from which the extent to which crystallization had continued on cooling can be seen—there is no difference between this image and the structure observed at 112 °C. The first stage of melting occurs at the crystal edges, with the disappearance of the knob marked A and the melting of the edges of the crystal marked B. Both of these areas crystallized on cooling from 127 °C. On further heating (Fig. 4(c)), the crystal continues to melt back from the edges, with melting still constrained to material that had crystallized below 127 °C. The rate of melting then rapidly increases, and there is melting across the whole of the sample in Fig. 4(d). However, note that the main flat on region of the crystal has not broken up into pieces, but rather is still melting back from the edges. There is a strikingly crystallographic shape (labelled C) in Fig. 4(d), although as this is the only time this sort of shape has been observed, it is possibly a coincidence. In Fig. 4(d), melting has revealed the dislocation branch (labelled D) that led to the formation of the lamella labelled A in Fig. 4a. Finally, by the time the sample has reached 136.3 °C (Fig. 4(e)) the crystals are starting to break up.

Fig. 5 shows the gradual melting of a sample isothermally crystallized at 124 °C ex situ and quenched to room temperature before melting in situ in the AFM. The area imaged is part of a spherulite, leading to the approximate alignment of the lamellae (radial direction from bottom right to top left). The series of images show a similar pattern to that in Fig. 4 above, with the initial melting of lamellae commencing at edges at low temperatures, followed eventually by more wide-scale melting with some lamellae appearing to break up into smaller sections. The arrowed areas A and B highlight initially flat on lamellae that can be seen to gradually melt back in successive images. The two-circled regions contain small stacks of lamellae that are edge-on to the surface. In this case, some of the lamellae in the stack disappear, but their neighbours appear to increase in thickness, although considering the pixel resolution (11 nm) this cannot be accurately measured. With further melting the image is dominated by a few large, flat-on crystals that have been revealed by the

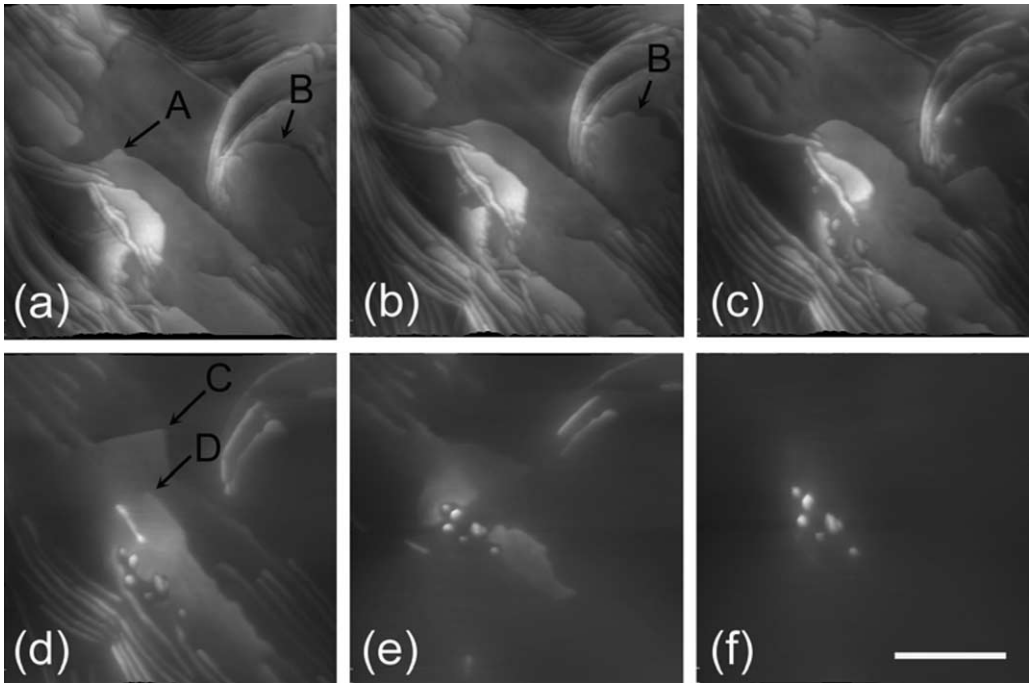

Fig. 4. A series of topographic AFM images showing the gradual melting of the aggregate shown in Fig. 3, following cooling to 112 °C. Heating rate 1 °C/min. The images have been tilted slightly to enhance contrast. (a) 124 °C, (b) 130.6 °C, (c) 132.9 °C, (d) 135.2 °C, (e) 136.3 °C, (f) 137.5 °C. Black to white represents 200 nm. The scale bar represents 1 μm.

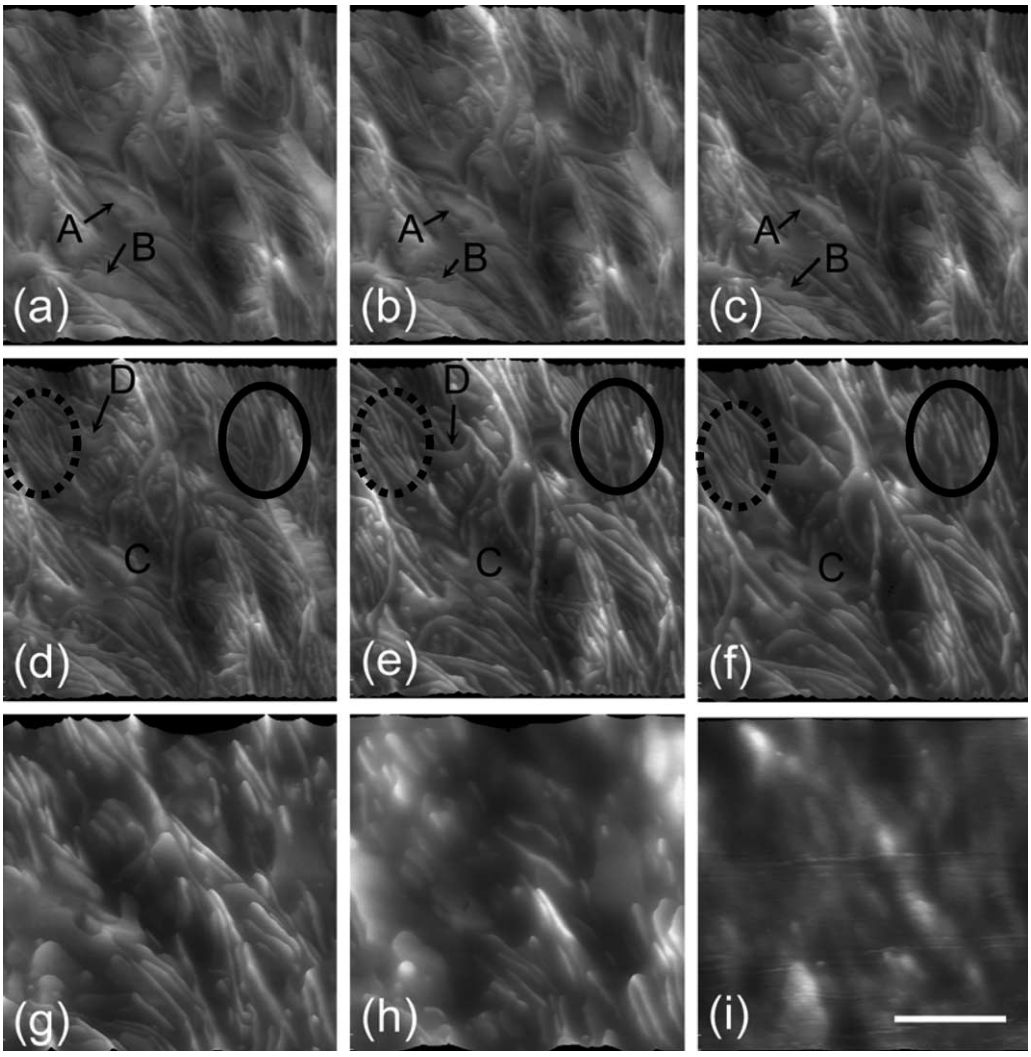

Fig. 5. A series of topographic AFM images showing the gradual melting of part of a spherulite that was crystallized isothermally at 124 °C. Heating rate 0.5 °C/min. The images have been tilted slightly to enhance contrast. (a) 124.6 °C, (b) 126.8 °C, (c) 128.8 °C, (d) 129.9 °C, (e) 131.0 °C, (f) 132.1 °C, (g) 134.4 °C, (h) 135.5 °C, (i) 143.8 °C. Black to white represents 150 nm. The scale bar represents 1 μm.

melting off of surface decoration. An example of such a flat-on crystal is labelled C. With further heating these also melt, again the process occurring back from the crystal edges.

Fig. 6 shows a similar data set of the melting of a sample quenched rapidly to room temperature from the melt so as to crystallize during rapid cooling. The formation of bands is clearly seen as the ridges running from top left to bottom right. In this case, the spherulite radius runs from top to bottom of the images. The much finer structure due to the rapid crystallization is clearly seen. On heating, again initial melting occurs back from the edges of flat-on crystals (arrowed A and B). However, this melting then leaves a largely edge-on population of crystals in contrast to the sample crystallized at higher temperature. These edge-on crystals do not extend for very long distances across the sample, most probably because their twisted morphology takes them below the sample surface. Further melting leads to these crystals shrinking in size and finally disappearing. Again there is a general impression that the crystal thickness is increasing with heating, but the pixel resolution is insufficient to quantify this.

Fig. 7 is a graph showing how the amount of crystalline material varies with temperature for the data sets shown in Figs. 4–6. The area of crystalline material was extracted using a thresh-holding method on the phase data (where there is a change in contrast between crystalline and amorphous material). The position of the thresh-hold was selected by eye, as the absolute phase difference between molten and crystalline material varied with temperature due to slight changes in the resonance properties of the cantilever with temperature that could not be corrected while still following the melting process in real time. All data sets are normalised by dividing through by the value of crystallinity before melting begun, as although realistic starting crystallinities were obtained from the data (66% for the 124 °C crystallized sample and 53% for the quenched sample), this is most probably a coincidence as there are always some dark areas (that would here be defined as molten) in the phase image of a rough surface. This normalisation allows the temperature dependence of the melting to be qualitatively compared, which is as much as can be reasonably obtained from data of this sort considering

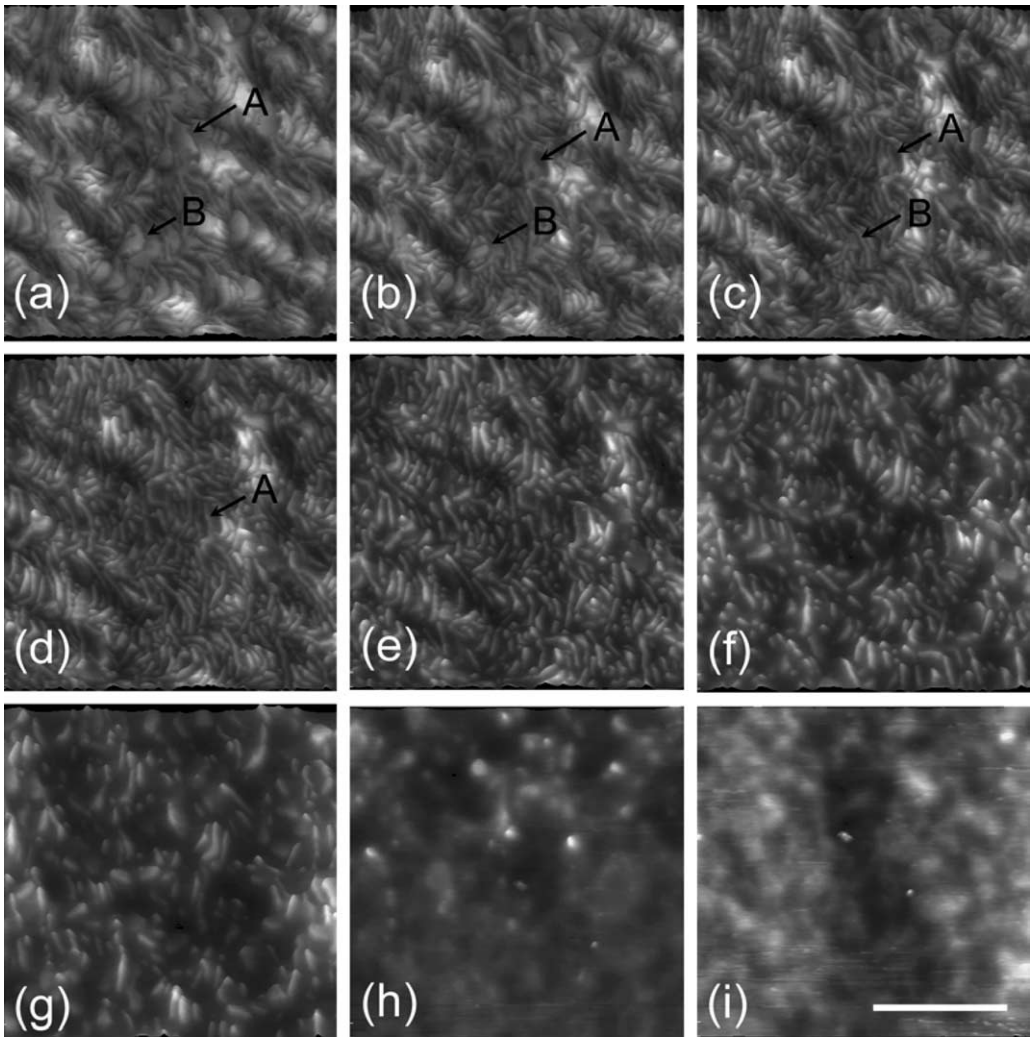

Fig. 6. A series of topographic AFM images showing the gradual melting of part of a spherulite that was crystallized on rapid quenching from the melt to room temperature. Heating rate 0.5 °C/min. The images have been tilted slightly to enhance contrast. (a) 124 °C, (b) 128.5 °C, (c) 129.7 °C, (d) 131.3 °C, (e) 132.3 °C, (f) 133.5 °C, (g) 134.6 °C, (h) 138.2 °C, (i) 139.4 °C. Black to white represents 100 nm. The scale bar represents 1 μm.

its semi-quantitative nature. Both the graphs for the spherulitic material show the expected gradual change in crystallinity over a temperature range of 12 °C. In the quenched sample the melting occurs continuously over this full temperature range, while the sample crystallized at 124 °C shows an initial melting, followed by a small plateau, and then a final rapid melting. The sample primarily crystallized at 127 °C shows much more rapid melting, although the heating rate in this sample is higher (1 °C/min compared to 0.5 °C/min).

4. Discussion

From all of the melting studies it is clear that melting occurs initially at the edges of crystals. This melting is not the reverse of crystallization, as the shapes of the melting lamellae are markedly different from those observed during in situ studies of polyethylene crystallization, with considerably more roughness and irregularity seen during melting. Here, melting is initiated at edges because of the increased mobility present at the edge of a crystal, rather than because of a difference in

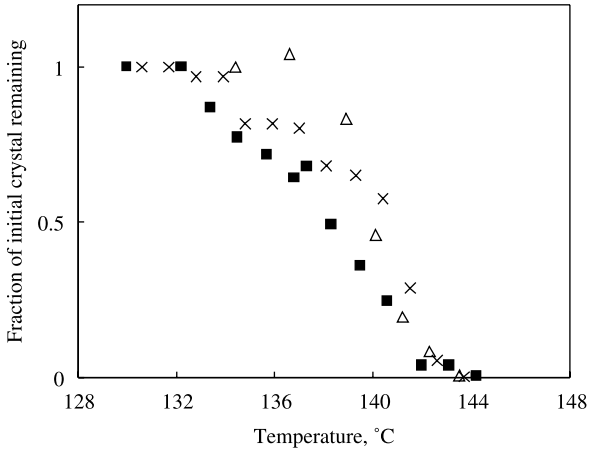

Fig. 7. A graph showing the total fraction of crystalline material present as a function of temperature for the data sets shown in Figs. 4–6, obtained by thresholding the phase data. The data has been normalised to start at 100% crystallinity for ease of comparison and due to the inability of the technique to measure low levels of molten material. ■ Sample crystallized on quenching, Δ sample crystallized in situ in the AFM at 127 °C, × sample crystallized isothermally ex situ at 124 °C.

stability of different parts of the crystal that depends on its age and therefore the extent to which it has been able to perfect. There is no evidence from our studies of lamellae melting by breaking up into blocks or similar fragments, as suggested in the model put forward in [22]. This conclusion is most clear in the images of lamellae that are flat-on in the surface of the sample, where the entirety of the crystal can be seen throughout the melting process. These conclusions are in agreement with those reached in [13], with the additional observations of the behaviour of flat-on lamellae that unambiguously confirms the result, and that continuous heating causes similar behaviour.

The data on melting of shish–kebab structures reveal several features of interest. Firstly, the most tightly packed crystals appear to melt most rapidly, for instance the one labelled A in Fig. 1. This is most probably due to the difficulty these crystals have in perfecting, as individual chains are shared between neighbouring crystals, and parts of chains are constrained through their attachment to neighbouring crystals. The existence of a so-called 'rigid amorphous' phase has been extensively discussed in the literature, e.g. [23], and this is most probably another example of its effect. It has also been suggested that such infilling lamellae contain the lower molecular weight fraction of material (see e.g. [24]) and that this will form less stable lamellae that will melt first. Again, this is direct, real-time confirmation of the inferences that have previously been drawn from ex situ study. Otherwise, although the crystals do not all melt at the same rate, there are no clear factors controlling the difference in melting rate of the different structures. As temperature is increased the lamellae melt back to the nucleating shish, which cannot be seen in Fig. 1, although a line of spots in the lower left of Fig. 1(f) reveal the location of the shish. Although, observing the extended chain shish is a rare event, as they are not usually on the sample surface, Fig. 2 shows the melting of a bundle of such structures. As expected, at low temperatures the shish are decorated by crystalline lamellae that have a somewhat elongated shape along the axis of the shish, in agreement with previous findings [25]. However, what is particularly striking here is the direct observation of the melting of these lamellar overgrowths, back from the radial direction so as to leave the most extended material behind. Finally, these are completely melted from the extended chain backbones, and the final figure shows the bare shish in situ, surrounded by molten polymer. These extended backbones melt more rapidly than the imaging technique can follow, which is not surprising considering their very high surface to volume ratio.

The observation that lamellae melt back from their ends, observed for the oriented samples, appears to present a contradiction with the fact that spherulites do not generally melt back along their radii, but rather gradually fade when viewed with an optical microscope. However, in the data on spherulite melting presented here, we see that melting still occurs from lamellar edges backwards, but that all of the lamellar edge surfaces are equally prone to melting, so the crystals melt in from the sides as well as back from the growth front.

The data shown in Fig. 4, in which both crystallization and melting were observed, confirms the expectation that the material crystallized at low temperatures will generally start to melt first. Again, the ability to observe both crystallization and melting in situ on the same sample allows unambiguous identification of the melting behaviour. Further heating and melting starts to remove the lamellae seen during initial crystallization, and reveal the underlying structure, such as the location of the dislocation branch that led to the formation of the lamella labelled A in Fig. 4(a). At the end of the series of images some dirt particles remain, which most probably caused the original nucleation of this structure. Strikingly though, during melting these particles actually appear to reduce the local stability of the crystals, as they melt free before the presumably later grown ends of the crystal have melted.

The way in which observation of the melting process can reveal initially hidden structures can also be seen in Fig. 5, where the melting back of the flat-on oriented lamella D reveals the presence of perpendicularly oriented crystals beneath it. It was not possible to observe crystallization of structures such as these in real time using AFM due to the very rapid growth rates that occur. However, these in situ melting experiments allow us to infer information about the initial growth of the sample in a similar manner to etching experiments traditionally carried out for electron microscopy [26], with the advantage that the progressive behaviour of the same area can be followed. The data shown for melting of a sample isothermally crystallized at 124 °C is part of a series of experiments performed at a range of isothermal crystallization temperatures from 118 to 127 °C, all of which showed similar behaviour. In all cases, melting reveals a coarsening of texture, with fine structure melting out first leaving primarily the larger lamellae behind. This fine structure that we see following a quench process could have either crystallized on cooling, or perhaps includes material that, due to later crystallization at the isothermal temperature, was more constrained and unable to perfect or contained less perfect and/or short chains. Figs. 1 and 4 reveal that both mechanisms can occur. The sample that was crystallized during a rapid quench melts in a slightly different way, with no bold underlying structure revealed, implying a much more isotropic stability across the entire crystal population.

The semi-quantitative analysis of the melting data given in Fig. 7 follows the expected behaviour, with a sharper melting transition in the high temperature isothermally crystallized sample than in the quenched sample. The corresponding data for the melting of the sample shown in Fig. 4, which was never quenched, gives an even sharper melting behaviour. This may be influenced by the particular morphology shown here, where the majority of the lamellae lie flat-on in the surface of the film, and so there is little available space for crystallization on cooling. It should be noted that the measured crystallinity here is a 'two-dimensional crystallinity' rather than the three-dimensional crystallinity measured by conventional techniques, and is therefore an indicative rather than an absolute measurement. However, the analysis shown here opens up the possibility of further quantitative studies relating the in situ melting behaviour with corresponding thermal analysis with DSC.

5. Conclusions

In situ observation of polyethylene melting with AFM provides a powerful tool to help extend the understanding gained through ex situ TEM studies.

Direct observation of extended chain oriented shish, with the melting off of the decorating lamellae observed in real-time, provides a convincing confirmation of our existing understanding of these structures.

In all cases, lamellae were observed to melt initially back from the crystal edges, with no observation of breaking up into fragments until close to complete melting of the sample. The edges of crystals, where chains naturally have the highest level of mobility, are the least stable, with no secondary structure within lamellae observed. However, melting is not the reverse of crystallization, with rough and complex morphologies seen at lamellar edges during melting.

The correlation of images with image analysis allows melting kinetics to be followed at both an individual crystal and crystal ensemble level, facilitating direct comparison with bulk techniques such as DSC or X-ray scattering.

References

[1] Bassett DC. Principles of polymer morphology Cambridge. Cambridge: Cambridge University Press; 1981.
[2] Bassett DC, Hodge AM. Proc R Soc London 1981;A377:25.
[3] Bassett DC, Hodge AM. Proc R Soc London 1981;A377:39.
[4] Bassett DC, Hodge AM. Proc R Soc London 1981;A377:61.
[5] Bassett DC, Patel D. Polymer 1994;35:1855.
[6] Toda A, Keller A. Colloid Polym Sci 1993;271:328.
[7] Hobbs JK, McMaster TJ, Miles MJ, Barham PJ. Polymer 1998;39(12): 2437.
[8] Pearce R, Vancso GJ. Polymer 1998;39:1237.
[9] Ivanov DA, Pop T, Yoon DY, Jonas AM. Macromolecules 2002;35(26): 9813.
[10] Li L, Chan C-M, Li J-X, Ng K-M, Yeung K-L, Weng L-T. Macromolecules 1999;32(24):8240.
[11] Loos J, Tian T. e-Polym 2002;36:1.
[12] Hobbs JK, Humphris ADL, Miles MJ. Macromolecules 2001;34:5508.
[13] Beekmans LGM, vand der Meer DW. Polymer 2002;43(6):1887.
[14] Winkel AK, Hobbs JK, Miles MJ. Polymer 2000;41(25):8791.
[15] Organ SJ, Hobbs JK, Miles MJ. Macromolecules 2004;37:4562.
[16] Tian M, Loos J. e-Polym 2003;51.
[17] Dubreuil N, Hocquet S, Dosiere M, Ivanov DA. Macromolecules 2004; 37(1):1.
[18] Hobbs JK, Chinese. J Polym Sci 2003;21(2):135.
[19] Hobbs JK. In: Sommer JU, Reiter G, editors. Polymer crystallization: observations, concepts and interpretations. Berlin: Springer; 2003. p. 82–95.
[20] Hobbs JK, Humphris ADL, Miles MJ. In: Batteas JD, Michaels CA, Walker GC, editors. Applications of scanned probe microscopy to polymers ACS Symposium Series 897, 2005;194.
[21] Horber JKH, Miles MJ. Science 2003;302(5647):1002.
[22] Strobl G. Eur Phys JE 2000;3:165.
[23] Schick C, Wurm A, Mohammed A. Thermochem Acta 2003;396(1–2): 119.
[24] Bassett DC. Philos Trans R Soc London, Ser A 1994;348:29.
[25] Odell JA, Keller A, Miles MJ. Coll Poly Sci 1984;262:683.
[26] Bassett DC. Macromol Symp 2004;214:5.